Vietnam Journal of Mechanics, Vol. 45, No. 4 (2023), pp. 296 – 317
DOI: https://doi.org/10.15625/0866-7136/19697

EXACT RECEPTANCE FUNCTION OF A TAPERED AFG BEAM WITH NONLINEARLY VARYING RATIOS OF BEAM PROPERTIES CARRYING CONCENTRATED MASSES

Thao Thi Bich Dao[1,2], **Khoa Viet Nguyen**[1,2,3,*], **Quang Van Nguyen**[1]
[1]*Institute of Mechanics, VAST, Hanoi, Vietnam*
[2]*Graduate University of Science and Technology, VAST, Hanoi, Vietnam*
[3]*VNU University of Engineering and Technology, Hanoi, Vietnam*
[*]E-mail: nvkhoa@imech.vast.vn

Received: 15 October 2023 / Revised: 27 December 2023 / Accepted: 29 December 2023
Published online: 31 December 2023

Abstract. This paper presents a method for establishing the exact receptance function of a tapered axially functionally graded (AFG) beam with nonlinear ratios of properties using the Adomian method. In current papers, the Adomian method was applied for linearly tapered beams where the geometric series was used conveniently. However, for nonuniform AFG beams with nonlinearly varying ratios of properties, the geometric series cannot be used, thus the other type of power series needs to be established and applied. In this paper, the derivation of the power series applied for obtaining the exact receptance function of a nonuniform AFG beam with nonlinearly varying ratios of properties is presented. Numerical simulation results of the receptance function of a tapered AFG beam with nonlinearly varying ratios of beam properties carrying concentrated masses are conducted and provided. The influences of the concentrated masses and the varying ratios of properties of beam on the receptance matrix are also investigated and presented.

Keywords: receptance, frequency response function, concentrated mass, functionally graded material beam.

1. INTRODUCTION

Frequency response function is used in many problems such as finite element model updating, vibration and noise control, system identification, structural damage detection, dynamic optimization, numerous mechanical, aerospace and civil engineering systems, etc. Mottershead et al. [1, 2] described the theory and practical application of the receptance method for vibration suppression in structures by multi-input partial pole placement and studied the measured zeros form frequency response functions and its

application to model assessment and updating. A new damage detection algorithm is formulated to utilize an original analytical model and FRF data measured prior and posterior to damage for structural damage detection is presented by Wang et al. [3]. Based on nonlinear perturbation equations of FRF data, an algorithm has been derived which can be used to determine a damage vector indicating both location and magnitude of damage from perturbation equations of FRF data. The frequency response function of a cantilevered beam, which is simply supported in-span is determined by Gürgöze and Erol [4]. In this work, the frequency response function is obtained through a formula, which was established for the receptance matrix of discrete systems subjected to linear constraint equations. Huang et al. [5] presented a new method for system identification and damage detection of controlled building structures equipped with semi-active friction dampers through model updating based on frequency response functions. The influence of the higher-order modes on the frequency response functions (FRFs) of non-proportionally viscously damped systems is eliminated by Li et al. [6]. In this study, two power-series expansions in terms of eigenpairs and system matrices are derived to obtain the FRF matrix based on the Neumann expansion theorem. Failla [7] concerned the frequency response analysis of beams and plane frames with an arbitrary number of Kelvin–Voigt viscoelastic dampers. The theory of generalised functions within a 1D formulation of equations of motion are used to derive the exact closed-form expressions for beam dynamic Green's functions and frequency response functions under arbitrary polynomial load, with arbitrary number of dampers. Nguyen [8] presented the general form of receptance functions of the isotropic homogeneous and axially functionally graded beams carrying concentrated masses and then compared the matrices of them. Singh et al. [9] presented a method for feedback control design using the receptance method is presented which can utilize the available partial measurements for control gain computation.

Non-uniform beams and concentrated mass are the two subjects concerned in studying the vibrations of the beam. Lenci et al. [10] used the asymptotic development method to obtain approximate analytical expressions for the natural frequencies of non-uniform cables and beams. In this work, some examples are reported to illustrate the effectiveness and simplicity of the proposed formulas. Eberle and Oberguggenberger [11] presented the bending stiffness curve of a non-uniform Euler-Bernoulli beam based on measured data from a static bending test and the calculus of variations. Hadian Jazi et al. [12] introduced an exact closed-form explicit solution for the transverse displacement of a non-uniform multi-cracked beam with any type of boundary conditions. A good agreement is evident when the obtained results are compared. An exact approach for free vibration analysis of a non-uniform beam with an arbitrary number of cracks and concentrated masses is proposed by Li [13]. By using the fundamental solutions and recurrence formulas, the mode shape function of vibration of a non-uniform beam with an arbitrary

number of cracks and concentrated masses are determined. Mahmoud [14,15] presented a general solution for the free transverse vibration of non-uniform, axially functionally graded cantilevers loaded at the tips with point masses. The free vibration analysis of non-uniform and stepped axially functionally graded (AFG) beams carrying arbitrary numbers of point masses is studied by using the Myklestad method. Tan et al. [16] presented an approach for free vibration analysis of the cracked non-uniform beam with general boundary conditions, whose mass per unit length and bending moment of inertia varying as polynomial functions.

In current published works, the receptance function of beam can be established using the Adomian method in which the receptance function is expressed as a geometric series - a special case of power series. In these publications the terms $(EI)'/EI$ and $(EI)''/EI$, where EI is a polynomial function, can be expressed easily as a geometric series. However, for nonuniform AFG beams with nonlinear ratios of properties these terms might not be expressed as a geometric series. In order to overcome this problem, we need to express these terms by another type of power series, not the geometric series.

The aim of this paper is to present a method for establishing the receptance function of a nonuniform AFG beam with nonlinear ratios of properties using the Adomian method where EI is an arbitrary polynomial function. In this paper, the derivation of the receptance function of a nonuniform AFG beam with nonlinearly ratios of properties is given in detail. The receptance function of a nonuniform AFG beam with nonlinearly ratios of properties and the influence of concentrated masses on that of the beam is investigated by numerical simulations. Numerical results show that the receptance matrices are changed when masses are attached on beam. When masses are attached at peak positions of the receptance matrices, these peaks will decrease significantly. The peaks and nodes of the receptance of the AFG beam move to the mass positions. These results can be useful for controlling the vibration amplitude of along the beam by using concentrated masses. Some new simulations of beam with nonlinearly ratios of properties of beam in this paper can be used for validating future works using other techniques.

2. THEORETICAL BACKGROUND

The modal of an axially tapered functionally graded beam is shown in Fig. 1. Assume that the elasticity modulus $E(x)$, inertia moment $I(x)$ and the mass density $\rho(x)$ of the beam are defined by

$$\begin{aligned} E(x) &= E_0\left(1-\alpha_1 x^{n_1}\right), \\ b(x) &= b_0\left(1-\alpha_2 x^{n_2}\right), \\ h(x) &= h_0\left(1-\alpha_3 x^{n_3}\right), \\ \rho(x) &= \rho_0\left(1-\alpha_4 x^{n_4}\right), \end{aligned} \tag{1}$$

where, E_0, b_0, h_0 and ρ_0 are Young's modulus, the width, the depth and mass density of beam at $x = 0$, respectively; $0 < \alpha_i < 1$; n_1, n_2 are the varying ratios of material properties.

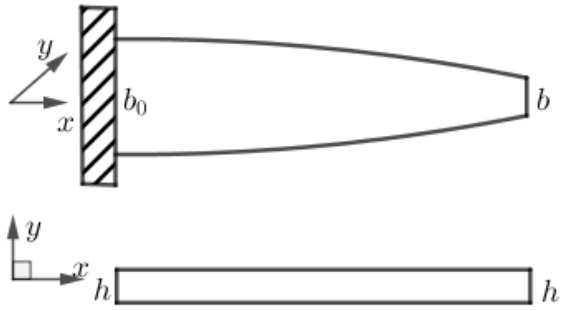

Fig. 1. The modal of an axially tapered functionally graded beam

The governing equation of bending vibration of an axially tapered functionally graded beam carrying concentrated masses can be presented as follows

$$\left[E\left(x\right)I\left(x\right)y''\right]'' + \left[\mu\left(x\right) + \sum_{k=1}^{n} m_k \delta\left(x - x_{mk}\right)\right]\ddot{y} = \delta\left(x - x_f\right) f\left(t\right), \tag{2}$$

where m_k is the k^{th} concentrated mass located at x_{mk}, $y(x, t)$ is the bending deflection of the beam at location x and time t, $f(t)$ is the force acting at position x_f, $\delta\left(x - x_f\right)$ is the Dirac delta function.

Using the notation $\xi = \dfrac{x}{L}$ which is non-dimensional coordinate, Eq. (2) can be rewritten in the form

$$\left[E\left(\xi\right)I\left(\xi\right)y''\right]'' + L^4\mu\left(\xi\right)\ddot{y} = L^4\delta\left(\xi - \xi_f\right) f\left(t\right) - L^4\sum_{k=1}^{n} m_k \delta\left(\xi - \xi_{mk}\right)\ddot{y}. \tag{3}$$

The receptance at ξ due to the force at ξ_f at the forcing frequency ω has the form

$$\alpha\left(\xi, \xi_f, \omega\right) = \mathbf{\Phi}^T\left(\xi\right)\left(\mathbf{K} - \omega^2\mathbf{M}\right)^{-1}\mathbf{\Phi}\left(\xi_f\right), \tag{4}$$

where

$$\mathbf{M} = \begin{bmatrix} \int_0^1 \mu\phi_1^2 \mathrm{d}\xi + \sum_{k=1}^{n} m_k\phi_1^2\left(\xi_{mk}\right) & \sum_{k=1}^{n} m_k\phi_1\left(\xi_{mk}\right)\phi_2\left(\xi_{mk}\right) & \cdots & \sum_{k=1}^{n} m_k\phi_1\left(\xi_{mk}\right)\phi_N\left(\xi_{mk}\right) \\ \sum_{k=1}^{n} m_k\phi_2\left(\xi_{mk}\right)\phi_1\left(\xi_{mk}\right) & \int_0^1 \mu\phi_2^2 \mathrm{d}\xi + \sum_{k=1}^{n} m_k\phi_2^2\left(\xi_{mk}\right) & \cdots & \sum_{k=1}^{n} m_k\phi_2\left(\xi_{mk}\right)\phi_N\left(\xi_{mk}\right) \\ \cdots & & & \cdots \\ \sum_{k=1}^{n} m_k\phi_N\left(\xi_{mk}\right)\phi_1\left(\xi_{mk}\right) & \sum_{k=1}^{n} m_k\phi_N\left(\xi_{mk}\right)\phi_2\left(\xi_{mk}\right) & \cdots & \int_0^1 \mu\phi_N^2 \mathrm{d}\xi + \sum_{k=1}^{n} m_k\phi_N^2\left(\xi_{mk}\right) \end{bmatrix},$$

$$\mathbf{K} = \frac{1}{L^4}\begin{bmatrix} \int_0^1 EI\phi''^2_1 \mathrm{d}\xi & 0 & ... & 0 \\ 0 & \int_0^1 EI\phi''^2_2 \mathrm{d}\xi & ... & 0 \\ ... & & & ... \\ 0 & 0 & ... & \int_0^1 EI\phi''^2_N \mathrm{d}\xi \end{bmatrix}, \tag{5}$$

$$\mathbf{\Phi}(\xi) = [\phi_1(\xi), ..., \phi_N(\xi)]^T, \ \ddot{\mathbf{q}}(t) = [\ddot{q}_1(t), ..., \ddot{q}_N(t)]^T, \ \mathbf{q}(t) = [q_1(t), ..., q_N(t)]^T,$$

and the term $\mathbf{\Phi}^T(\xi)\,\bar{\mathbf{q}}$ and $\bar{f}$ are the amplitudes of the response at ξ and the force at ξ_f, respectively.

In order to derive formula (4), the mode shape ϕ of the beam without attached masses needs to be determined. Any mode shape ϕ is determined by solving the eigenvalue problem of Eq. (3)

$$\left[E(\xi) I(\xi) \phi_i''(\xi)\right]'' - L^4\omega^2\mu(\xi)\phi_i(\xi) = 0. \tag{6}$$

Using the rules of differentiation, yields

$$\phi_i'''' = -\frac{2(EI)'}{EI}\phi_i''' - \frac{(EI)''}{EI}\phi_i'' + \frac{L^4\omega^2\mu}{EI}\phi_i,$$

or

$$\phi_i'''' = -\frac{2(EI)'}{EI}\phi_i''' - \frac{(EI)''}{EI}\phi_i'' + \frac{\lambda^2(1-\alpha_3\xi^{n_2})}{1-\alpha_1\xi^{n_1}}\phi_i, \tag{7}$$

where $\lambda^2 = \dfrac{\omega^2\mu_0 L^4}{E_0 I_0}$.

Applying the Adomian decomposition method, any mode shape ϕ is decomposed into the infinite sum of convergent series

$$\phi_i(\xi) = \sum_{k=0}^{\infty} C_k\xi^k. \tag{8}$$

By using the linear operators $\ell = \dfrac{\mathrm{d}^4}{\mathrm{d}\xi^4}$ and $\ell^{-1} = \int_0^\xi\int_0^\xi\int_0^\xi\int_0^\xi (...)\mathrm{d}\xi\mathrm{d}\xi\mathrm{d}\xi\mathrm{d}\xi$, we have

$$\phi_i(\xi) = C_0 + C_1\xi + C_2\xi^2 + C_3\xi^3 + l^{-1}\left(\phi_i''''\right),$$

or,

$$\phi_i = \sum_{k=0}^{3} C_k\xi^k + l^{-1}\left[-\frac{2(EI)'}{EI}\phi_i''' - \frac{(EI)''}{EI}\phi_i'' + \frac{\lambda^2(1-\alpha_3\xi^{n_2})}{1-\alpha_1\xi^{n_1}}\phi_i\right]. \tag{9}$$

Since EI is the polynomial function so the terms $\frac{(EI)'}{EI}$ and $\frac{(EI)''}{EI}$ are the rational fraction. From the partial fraction decomposition theory, a fraction of two polynomials $\frac{P(x)}{Q(x)}$ can be expressed in general form as follows

$$\frac{P(\xi)}{Q(\xi)} = \sum_k \frac{A_k}{(\xi - a)^k} + \sum_k \frac{B_k x + C_k}{(\xi^2 + b\xi + c)^k}. \tag{10}$$

If the partial fractions of terms $\frac{(EI)'}{EI}$ and $\frac{(EI)''}{EI}$ consist of only $\sum_k \frac{A_k}{(\xi - a)^k}$ then these partial fractions can be expressed by geometric series

$$\frac{A_k}{(\xi - a)^k} = \sum_{i=0}^{\infty} \tilde{A}_k \tilde{\xi}^i, \text{ where } \tilde{\xi} = \frac{\xi}{a}. \tag{11}$$

However, if those partial fractions include $\sum_k \frac{B_k x + C_k}{(\xi^2 + b\xi + c)^k}$ then they cannot be expressed simply as a geometric series. Let us consider an axially tapered AFG beam with nonlinearly varying width as follows

$$\begin{aligned} E(\xi) &= E_0 (1 - \alpha_1 \xi^{n_1}), \\ b &= b_0 (1 - \alpha_2 \xi^3), \\ h &= h_0, \\ \rho &= \rho_0 (1 - \alpha_4 \xi^{n_4}). \end{aligned} \tag{12}$$

In this case, the moment of inertia is expressed as the third polynomial function $I = I_0 (1 - \alpha_2 \xi^3)$, then

$$\begin{aligned} \frac{(EI)'}{EI} &= -\left[n_1 \alpha_1 \xi^{n_1 - 1} + 3\alpha_2 \xi^2 - (n_1 + 3)\alpha_1 \alpha_2 \xi^{n_1 + 2}\right] \frac{1}{(1 - \alpha_1 \xi^{n_1})(1 - \alpha_2 \xi^3)}, \\ \frac{(EI)''}{EI} &= -\left[n_1 (n_1 - 1)\alpha_1 \xi^{n_1 - 2} + 6\alpha_2 \xi - (n_1 + 3)(n_1 + 2)\alpha_1 \alpha_2 \xi^{n_1 + 1}\right] \frac{1}{(1 - \alpha_1 \xi^{n_1})(1 - \alpha_2 \xi^3)}, \end{aligned} \tag{13}$$

in which,

$$\frac{1}{(1 - \alpha_1 \xi^{n_1})(1 - \alpha_2 \xi^3)} = \frac{1}{3} \frac{1}{\left[1 - (\beta_1 \xi)^{n_1}\right]} \left[\frac{1}{1 - \beta_2 \xi} + \frac{\beta_2 \xi + 2}{1 + \beta_2 \xi + \beta_2^2 \xi^2}\right], \tag{14}$$

where $\beta_1 = \sqrt[n_1]{\alpha_1}, \beta_2 = \sqrt[3]{\alpha_2}$ with the assumption that $\beta_i \xi < 1, i = 1, 2, 3, 4$.

The following terms in (14) can be expressed by geometric series

$$\begin{aligned}\frac{1}{1-(\beta_1\xi)^{n_1}} &= \sum_{k=0}^{\infty}\alpha_1\xi^{kn_1},\\ \frac{1}{1-\beta_2\xi} &= \sum_{k=0}^{\infty}\alpha_2\xi^{k}.\end{aligned} \tag{15}$$

However, the second term in the bracket cannot be expressed in term of geometric series. Thus, we will express this term as a power series using another method as follows.

Since $\beta_i\xi < 1, i = 1,2$, using the power series one can obtain

$$\frac{1}{1+\beta_2\xi+\beta_2^2\xi^2} = \sum_{u=0}^{\infty}A_u\xi^u \text{ with } \begin{cases} A_0 = 1\\ A_1 = -\beta_2\\ A_u = -\beta_2 A_{u-1} - \beta_2^2 A_{u-2},\ u \geq 2\end{cases} \tag{16}$$

The coefficients of this can be expressed as

$$A_0 = 1,\ A_1 = -\beta_2,\ A_2 = 0,\ A_3 = \beta_2^3,\ A_4 = -\beta_2^4,\ A_5 = 0,\ A_6 = \beta_2^6, ...$$

Therefore,

$$\begin{aligned}\frac{1}{1+\beta_2\xi+\beta_2^2\xi^2} &= \sum_{u=0}^{\infty}C_u\xi^u = \xi^0 - \beta_2^1\xi^1 + \beta_2^3\xi^3 - \beta_2^4\xi^4 + \beta_2^6\xi^6 - \beta_2^7\xi^7 + ...\\ &= \sum_{n=0}^{\infty}(-1)^n b_n, \quad 0 \leq b_n < 1.\end{aligned} \tag{17}$$

This is a converged alternating series since it satisfies the convergence conditions of an alternating series

$$\begin{cases} b_{n+1} < b_n,\ \forall n\\ \lim\limits_{n\to\infty} b_n = 0\end{cases} \tag{18}$$

Applying Cauchy product, one has

$$\begin{aligned}\frac{1}{(1-\alpha_1\xi^{n_1})(1-\alpha_2\xi^3)} &= \sum_{u=0}^{\infty}\left(\beta_1^{n_1}\xi^{n_1}\right)^u\frac{1}{3}\left[\sum_{v=0}^{\infty}(\beta_2\xi)^v + (\beta_2\xi+2)\sum_{v=0}^{\infty}A_v\xi^v\right]\\ &= \frac{1}{3}\left[\sum_{i=0}^{\infty}B_{1i}\xi^i + (\beta_2\xi+2)\sum_{i=0}^{\infty}B_{1i}\xi^i\right],\end{aligned} \tag{19}$$

where

$$B_{1i} = \sum_{j=0}^{m_1}\beta_1^{n_1 j}\beta_2^{i-n_1 j}, \quad B_{2i} = \sum_{j=0}^{m_1}\beta_1^{n_1 j}A_{i-n_1 j}, \quad m_1 = \left[\frac{i}{n_1}\right], \tag{20}$$

in which $m_1 = \left[\frac{i}{n_1}\right]$ is the largest integer that is less than or equal to $\frac{i}{n_1}$, p is the remainder of $\frac{i}{n_1}$, and

$$\begin{aligned}
\frac{\phi_i'''}{(1-\alpha_1\xi^{n_1})(1-\alpha_2\xi^3)} &= \frac{1}{3}\left[\sum_{v=0}^{\infty}(\beta_2\xi)^v + (\beta_2\xi+2)\sum_{v=0}^{\infty}A_v\xi^v\right].\sum_{l=0}^{\infty}(l+1)(l+2)(l+3)C_{l+3}\xi^l \\
&= \frac{1}{3}\left[\sum_{i=0}^{\infty}\xi^i\sum_{j=0}^{i}B_{1i}(i-j+1)(i-j+2)(i-j+3)C_{i-j+3}\right. \\
&\quad \left. + (\beta_2\xi+2)\sum_{i=0}^{\infty}\xi^i\sum_{j=0}^{i}B_{2i}(i-j+1)(i-j+2)(i-j+3)C_{i-j+3}\right], \\
\frac{\phi_i''}{(1-\alpha_1\xi^{n_1})(1-\alpha_2\xi^3)} &= \frac{1}{3}\left[\sum_{v=0}^{\infty}(\beta_2\xi)^v + (\beta_2\xi+2)\sum_{v=0}^{\infty}A_v\xi^v\right].\sum_{l=0}^{\infty}(l+1)(l+2)C_{l+2}\xi^l \\
&= \frac{1}{3}\left[\sum_{i=0}^{\infty}\xi^i\sum_{j=0}^{i}B_{1i}(i-j+1)(i-j+2)C_{i-j+2}\right. \\
&\quad \left. + (\beta_2\xi+2)\sum_{i=0}^{\infty}\xi^i\sum_{j=0}^{i}B_{2i}(i-j+1)(i-j+2)C_{i-j+2}\right], \\
\frac{\phi_i}{\left[1-(\beta_1\xi)^{n_1}\right]} &= \sum_{u=0}^{\infty}(\beta_1\xi)^{n_1u}.\sum_{v=0}^{\infty}C_v\xi^v = \sum_{i=0}^{\infty}\xi^i\sum_{j=0}^{m_1}\beta_1^{nj}C_{i-nj}.
\end{aligned} \tag{21}$$

Substituting Eqs. (21) and (13) into Eq. (7), yields

$$\begin{aligned}
\phi_i'''' = \frac{2}{3}\Bigg[&\sum_{i=0}^{\infty}\xi^{i+n_1-1}\sum_{j=0}^{i}(B_{1i}+2B_{2i})n_1\alpha_1(i-j+1)(i-j+2)(i-j+3)C_{i-j+3} \\
&+\sum_{i=0}^{\infty}\xi^{i+n_1}\sum_{j=0}^{i}B_{2i}n_1\alpha_1\beta_2(i-j+1)(i-j+2)(i-j+3)C_{i-j+3} \\
&+\sum_{i=0}^{\infty}\xi^{i+2}\sum_{j=0}^{i}(B_{1i}+2B_{2i})3\alpha_2(i-j+1)(i-j+2)(i-j+3)C_{i-j+3} \\
&+\sum_{i=0}^{\infty}\xi^{i+3}\sum_{j=0}^{i}B_{2i}3\alpha_2\beta_2(i-j+1)(i-j+2)(i-j+3)C_{i-j+3} \\
&-\sum_{i=0}^{\infty}\xi^{i+n_1+2}\sum_{j=0}^{i}(B_{1i}+2B_{2i})(n_1+3)\alpha_1\alpha_2(i-j+1)(i-j+2)(i-j+3)C_{i-j+3} \\
&-\sum_{i=0}^{\infty}\xi^{i+n_1+3}\sum_{j=0}^{i}B_{2i}(n_1+3)\alpha_1\alpha_2\beta_2(i-j+1)(i-j+2)(i-j+3)C_{i-j+3}\Bigg]
\end{aligned} \tag{22}$$

$$
\begin{aligned}
&+\frac{1}{3}\left[\sum_{i=0}^{\infty}\xi^{i+n_1-2}\sum_{j=0}^{i}\left(B_{1i}+2B_{2i}\right)\alpha_1 n_1\left(n_1-1\right)\left(i-j+1\right)\left(i-j+2\right)C_{i-j+2}\right.\\
&+\sum_{i=0}^{\infty}\xi^{i+n_1-1}\sum_{j=0}^{i}B_{2i}\alpha_1\beta_2 n_1\left(n_1-1\right)\left(i-j+1\right)\left(i-j+2\right)C_{i-j+2}\\
&+\sum_{i=0}^{\infty}\xi^{i+1}\sum_{j=0}^{i}\left(B_{1i}+2B_{2i}\right)6\alpha_2\left(i-j+1\right)\left(i-j+2\right)C_{i-j+2}\\
&+\sum_{i=0}^{\infty}\xi^{i+2}\sum_{j=0}^{i}B_{2i}6\alpha_2\beta_2\left(i-j+1\right)\left(i-j+2\right)C_{i-j+2}\\
&-\sum_{i=0}^{\infty}\xi^{i+n_1+1}\sum_{j=0}^{i}\left(B_{1i}+2B_{2i}\right)\alpha_1\alpha_2\left(n_1+2\right)\left(n_1+3\right)\left(i-j+1\right)\left(i-j+2\right)C_{i-j+2}\\
&\left.-\sum_{i=0}^{\infty}\xi^{i+n_1+2}\sum_{j=0}^{i}B_{2i}\alpha_1\alpha_2\beta_2\left(n_1+2\right)\left(n_1+3\right)\left(i-j+1\right)\left(i-j+2\right)C_{i-j+2}\right],\\
&-\sum_{i=0}^{\infty}\xi^{i+n_2}\sum_{j=0}^{\left[\frac{i}{n_1}\right]}\lambda^2\alpha_3\beta_1^{n_1 j}C_{i-n_1 j}+\sum_{i=0}^{\infty}\xi^{i}\sum_{j=0}^{\left[\frac{i}{n_1}\right]}\lambda^2\beta_1^{n_1 j}C_{i-n_1 j}.
\end{aligned}
$$

Plugging Eq. (22) into Eq. (9) and implementing the integration operator in Eq. (9), we have:

$$
\begin{aligned}
\phi_i=&\sum_{k=0}^{3}C_k\xi^k+\frac{2}{3}n_1\alpha_1\sum_{k=0}^{\infty}\xi^{k+n_1+3}\frac{\sum_{i=0}^{i}\left(B_{1i}+2B_{2i}\right)\left(k-i+1\right)\left(k-i+2\right)\left(k-i+3\right)C_{k-i+3}}{\left(k+n_1\right)\left(k+n_1+1\right)\left(k+n_1+2\right)\left(k+n_1+3\right)}\\
&+\frac{2}{3}n_1\alpha_1\beta_2\sum_{k=0}^{\infty}\xi^{k+n_1+4}\frac{\sum_{i=0}^{i}B_{2i}\left(k-i+1\right)\left(k-i+2\right)\left(k-i+3\right)C_{k-i+3}}{\left(k+n_1+1\right)\left(k+n_1+2\right)\left(k+n_1+3\right)\left(k+n_1+4\right)}\\
&+2\alpha_2\sum_{k=0}^{\infty}\xi^{k+6}\frac{\sum_{i=0}^{i}\left(B_{1i}+2B_{2i}\right)\left(k-i+1\right)\left(k-i+2\right)\left(k-i+3\right)C_{k-i+3}}{\left(k+3\right)\left(k+4\right)\left(k+5\right)\left(k+6\right)}\\
&+2\alpha_2\beta_2\sum_{k=0}^{\infty}\xi^{k+7}\frac{\sum_{i=0}^{i}B_{2i}\left(k-i+1\right)\left(k-i+2\right)\left(k-i+3\right)C_{k-i+3}}{\left(k+4\right)\left(k+5\right)\left(k+6\right)\left(k+7\right)}\\
&-\frac{2}{3}\left(n_1+3\right)\alpha_1\alpha_2\sum_{k=0}^{\infty}\xi^{k+n_1+6}\frac{\sum_{i=0}^{i}\left(B_{1i}+2B_{2i}\right)\left(k-i+1\right)\left(k-i+2\right)\left(k-i+3\right)C_{k-i+3}}{\left(k+n_1+3\right)\left(k+n_1+4\right)\left(k+n_1+5\right)\left(k+n_1+6\right)}\\
&-\frac{2}{3}\left(n_1+3\right)\alpha_1\alpha_2\beta_2\sum_{k=0}^{\infty}\xi^{k+n_1+7}\frac{\sum_{i=0}^{i}B_{2i}\left(k-i+1\right)\left(k-i+2\right)\left(k-i+3\right)C_{k-i+3}}{\left(k+n_1+4\right)\left(k+n_1+5\right)\left(k+n_1+6\right)\left(k+n_1+7\right)}
\end{aligned}
\tag{23}
$$

$$+\frac{1}{3}\alpha_1 n_1\left(n_1-1\right)\sum_{k=0}^{\infty}\xi^{k+n_1+2}\frac{\sum_{i=0}^{k}\left(B_{1i}+2B_{2i}\right)\left(k-i+1\right)\left(k-i+2\right)C_{k-i+2}}{\left(k+n_1-1\right)\left(k+n_1\right)\left(k+n_1+1\right)\left(k+n_1+2\right)}$$

$$+\frac{1}{3}\alpha_1\beta_2 n_1\left(n_1-1\right)\sum_{k=0}^{\infty}\xi^{k+n_1+3}\frac{\sum_{i=0}^{k}B_{2i}\left(k-i+1\right)\left(k-i+2\right)C_{k-i+2}}{\left(k+n_1\right)\left(k+n_1+1\right)\left(k+n_1+2\right)\left(k+n_1+3\right)}$$

$$+2\alpha_2\sum_{k=0}^{\infty}\xi^{k+5}\frac{\sum_{i=0}^{k}\left(B_{1i}+2B_{2i}\right)\left(k-i+1\right)\left(k-i+2\right)C_{k-i+2}}{\left(k+2\right)\left(k+3\right)\left(k+4\right)\left(k+5\right)}$$

$$+2\alpha_2\beta_2\sum_{k=0}^{\infty}\xi^{k+6}\frac{\sum_{j=0}^{i}B_{2i}\left(k-i+1\right)\left(k-i+2\right)C_{k-i+2}}{\left(k+3\right)\left(k+4\right)\left(k+5\right)\left(k+6\right)}$$

$$-\frac{1}{3}\alpha_1\alpha_2\left(n_1+2\right)\left(n_1+3\right)\sum_{k=0}^{\infty}\xi^{k+n_1+5}\frac{\sum_{j=0}^{i}\left(B_{1i}+2B_{2i}\right)\left(k-i+1\right)\left(k-i+2\right)C_{k-i+2}}{\left(k+n_1+2\right)\left(k+n_1+3\right)\left(k+n_1+4\right)\left(k+n_1+5\right)}$$

$$-\frac{1}{3}\alpha_1\alpha_2\beta_2\left(n_1+2\right)\left(n_1+3\right)\sum_{k=0}^{\infty}\xi^{k+n_1+6}\frac{\sum_{j=0}^{i}B_{2i}\left(k-i+1\right)\left(k-i+2\right)C_{k-i+2}}{\left(k+n_1+3\right)\left(k+n_1+4\right)\left(k+n_1+5\right)\left(k+n_1+6\right)}$$

$$-\lambda^2\alpha_3\sum_{k=0}^{\infty}\xi^{k+n_2+4}\frac{\sum_{i=0}^{\left[\frac{k}{n_1}\right]}\beta_1^{n_1 i}C_{k-n_1 i}}{\left(k+n_2+1\right)\left(k+n_2+2\right)\left(k+n_2+3\right)\left(k+n_2+4\right)}$$

$$+\lambda^2\sum_{k=0}^{\infty}\xi^{k+4}\frac{\sum_{i=0}^{\left[\frac{k}{n_1}\right]}\beta_1^{n_1 i}C_{k-n_1 i}}{\left(k+1\right)\left(k+2\right)\left(k+3\right)\left(k+4\right)}.$$

The coefficients C_k where $k<4$ can be determined from the boundary conditions. Let us consider a simply supported beam, the boundary conditions can be expressed as:

$$\phi(0)=0,\quad \phi''(0)=0, \tag{24}$$

$$\phi(1)=0,\quad \phi''(1)=0. \tag{25}$$

From Eqs. (24) and (25) we have

$$C_0=0,\ C_1\neq 0,\ C_2=0,\ C_3\neq 0. \tag{26}$$

For $k\geq 4$ the coefficients C_k can be calculated from the recurrent relations depending on the value of n_1 as follows

$$
\begin{aligned}
C_k = {} & \frac{2}{3} n_1 \alpha_1 \frac{\sum_{i=0}^{k-n_1-3} (B_{1i} + 2B_{2i}) (k-n_1-i-2) (k-n_1-i-1) (k-n_1-i) C_{k-n_1-i}}{(k-3)(k-2)(k-1)k} \\
& + \frac{2}{3} n_1 \alpha_1 \beta_2 \frac{\sum_{i=0}^{k-n_1-4} B_{2i} (k-n_1-i-3) (k-n_1-i-2) (k-n_1-i-1) C_{k-n_1-i-1}}{(k-3)(k-2)(k-1)k} \\
& + 2\alpha_2 \frac{\sum_{i=0}^{k-6} (B_{1i} + 2B_{2i}) (k-i-5) (k-i-4) (k-i-3) C_{k-i-3}}{(k-3)(k-2)(k-1)k} \\
& + 2\alpha_2 \beta_2 \frac{\sum_{i=0}^{k-7} B_{2i} (k-i-6) (k-i-5) (k-i-4) C_{k-i-4}}{(k-3)(k-2)(k-1)k} \\
& - \frac{2}{3} (n_1+3) \alpha_1 \alpha_2 \frac{\sum_{i=0}^{k-n_1-6} (B_{1i} + 2B_{2i}) (k-n_1-i-5) (k-n_1-i-4) (k-n_1-i-3) C_{k-n_1-i-3}}{(k-3)(k-2)(k-1)k} \\
& - \frac{2}{3} (n_1+3) \alpha_1 \alpha_2 \beta_2 \frac{\sum_{i=0}^{k-n_1-7} B_{2i} (k-n_1-i-6) (k-n_1-i-5) (k-n_1-i-4) C_{k-n_1-i-4}}{(k-3)(k-2)(k-1)k} \\
& + \frac{1}{3} \alpha_1 n_1 (n_1-1) \frac{\sum_{i=0}^{k-n_1-2} (B_{1i} + 2B_{2i}) (k-n_1-i-1) (k-n_1-i) C_{k-n_1-i}}{(k-3)(k-2)(k-1)k} \\
& + \frac{1}{3} \alpha_1 \beta_2 n_1 (n_1-1) \frac{\sum_{i=0}^{k-n_1-3} B_{2i} (k-n_1-i-2) (k-n_1-i-1) C_{k-n_1-i-1}}{(k-3)(k-2)(k-1)k} \\
& + 2\alpha_2 \frac{\sum_{i=0}^{k-5} (B_{1i} + 2B_{2i}) (k-i-4) (k-i-3) C_{k-i-3}}{(k-3)(k-2)(k-1)k} \\
& + 2\alpha_2 \beta_2 \frac{\sum_{i=0}^{k-6} B_{2i} (k-i-5) (k-i-4) C_{k-i-4}}{(k-3)(k-2)(k-1)k} \\
& - \frac{1}{3} \alpha_1 \alpha_2 (n_1+2)(n_1+3) \frac{\sum_{i=0}^{k-n_1-5} (B_{1i} + 2B_{2i}) (k-n_1-i-4) (k-n_1-i-3) C_{k-n_1-i-3}}{(k-3)(k-2)(k-1)k} \\
& - \frac{1}{3} \alpha_1 \alpha_2 \beta_2 (n_1+2)(n_1+3) \frac{\sum_{i=0}^{k-n_1-6} (B_{1i} + 2B_{2i}) (k-n_1-i-5) (k-n_1-i-4) C_{k-n_1-i-4}}{(k-3)(k-2)(k-1)k} \\
& - \lambda^2 \alpha_3 \frac{\sum_{i=0}^{\left[\frac{k-n_2-4}{n_1}\right]} \beta_1^{n_1 i} C_{k-n_2-n_1 i-4}}{(k-3)(k-2)(k-1)k} + \lambda^2 \frac{\sum_{i=0}^{\left[\frac{k-4}{n_1}\right]} \beta_1^{n_1 i} C_{k-n_1 i-4}}{(k-3)(k-2)(k-1)k}. \qquad (27)
\end{aligned}
$$

Therefore, ϕ_i in Eq. (23) can be expressed as a linear function of C_1 and C_3. Since coefficients C_k are determined from the recurrent equation (27), the coefficients C_k are the functions of C_1, C_3 and λ, thus ϕ_i is also a function of C_1, C_3 and λ.

By substituting Eq. (27) into Eq. (24)–(25), we have

$$\sum_{k=0}^{\infty} C_k = 0 \Leftrightarrow f_{11}(\lambda)C_1 + f_{12}(\lambda)C_3 = 0, \tag{28}$$

$$\sum_{k=0}^{\infty} (k+1)\, C_{k+1} = 0 \Leftrightarrow f_{21}(\lambda)C_1 + f_{22}(\lambda)C_3 = 0. \tag{29}$$

In order to have non-trivial C_1 and C_3 of Eqs. (28) and (29), the following condition must be satisfied

$$f_{11}(\lambda)f_{22}(\lambda) - f_{12}(\lambda)f_{21}(\lambda) = 0. \tag{30}$$

Solving Eq. (30), the dimensionless frequency λ_i will be determined. Substituting the solution λ_i into Eqs. (28), C_3 can be calculated as the function of a given C_1

$$C_3 = -\frac{f_{11}(\lambda)}{f_{12}(\lambda)}C_1. \tag{31}$$

The n^{th} mode shape ϕ_n corresponding to λ_n is calculated from Eq. (23). Once the mode shape ϕ_i is determined, the following relations is derived

$$\phi_i^2(\xi) = \sum_{k=0}^{\infty} C_k\xi^k \sum_{k=0}^{\infty} C_k\xi^k = \sum_{k=0}^{\infty} \xi^k \sum_{i=0}^{k} C_{k-i}C_i, \tag{32}$$

$$\begin{aligned} \phi_i''^2(\xi) &= \sum_{k=0}^{\infty} C_k\xi^k (k+1)(k+2) \sum_{k=0}^{\infty} C_k\xi^k (k+1)(k+2) \\ &= \sum_{k=0}^{\infty} \xi^k \sum_{i=0}^{k} C_{k-i+2}C_{i+2} (i+1)(i+2)(k-i+1)(k-i+2) \end{aligned} \tag{33}$$

$$\begin{aligned} \int_0^1 \mu\phi_i^2 \mathrm{d}\xi &= \int_0^1 \mu_0 (1-\alpha_2\xi^n) \sum_{k=0}^{\infty} \xi^k \sum_{i=0}^{k} C_{k-i}C_i \mathrm{d}\xi \\ &= \sum_{k=1}^{\infty} \frac{\mu_0 [(k+1)(1-\alpha_2)+n+1]}{(k+1)(k+n+1)} \sum_{i=0}^{k} C_{k-i}C_i, \end{aligned} \tag{34}$$

$$\int_0^1 IE\phi''^2_i d\xi =$$
$$= \int_0^1 IE_0\left(1-\alpha_1\xi^n\right)\sum_{k=0}^{\infty}\xi^k\sum_{i=0}^{k}C_{k-i+2}C_{i+2}\left(i+1\right)\left(i+2\right)\left(k-i+1\right)\left(k-i+2\right)d\xi$$
$$= \sum_{k=1}^{\infty}\frac{IE_0\left[\left(k+1\right)\left(1-\alpha_1\right)+n+1\right]}{\left(k+1\right)\left(k+n+1\right)}\sum_{i=0}^{k}C_{k-i+2}C_{i+2}\left(i+1\right)\left(i+2\right)\left(k-i+1\right)\left(k-i+2\right). \tag{35}$$

Substituting Eqs. (32)–(35) into Eq. (5) the matrices **M** and **K** and the receptance formula (4) will be determined.

3. NUMERICAL SIMULATION

3.1. Reliability of the theory

To justify the formula of receptance function for the AFG beam, a cantilever beam consisting of two constituent materials of aluminum and zirconia presented in [14] is applied. The material properties are E_{Al} = 70 GPa, ρ_{Al} = 2702 kg/m^3 for aluminum, and E_z = 200 GPa, and ρ_z = 5700 kg/m^3 for zirconia. Frequency parameters were obtained using $\Omega_i = \dfrac{\omega_i L^2}{h^2}\sqrt{\dfrac{12\rho_s}{E_s}}$. To examine the convergence of the solution, a cantilever beam with the material properties varying linearly when ratio n = 1 is considered. The coefficients C_k can be approximated by the N-term truncated series, Eq. (17) can be expressed as

$$\phi\left(\xi\right) = \sum_{k=0}^{N} C_k\xi^k. \tag{36}$$

Calculations show that when the 100-term truncated series in Eq. (36) is applied the following condition is met

$$\left|\Omega_1^N - \Omega_1^{N-1}\right| < \varepsilon = 6.055E{-}10. \tag{37}$$

Table 1. Frequency parameter of the cantilever AFG beam

Case	Frequency parameter	Ref. [14]	Present paper	Error (%)
Alumina-Zirconia	Ω_1	5.888	5.888	0
	Ω_2	26.060	26.060	0
	Ω_3	64.939	64.941	0.003080
	Ω_4	122.532	122.531	0.000816
	Ω_5	199.075	199.176	0.050710

Therefore, the series summation limit N in Eq. (37) will be truncated to $N = 100$ in all the calculations in this work. Five lowest frequency parameters of the cantilever AFG beam obtained by two methods are listed in Table 1.

The excellent agreement of the frequency parameters between the present work and Ref. [14] presented in Table 1 verifies the reliability of the proposed method.

3.2. Influence of the varying properties of material on the receptance

Fig. 2 presents the 3D graphs of receptance of the simply supported beam in two cases: $n_2 = 1$ and $n_2 = 3$ when the forcing frequencies equal to the first, the second and the third natural frequencies of beam, respectively. Figs. 2(a), 2(c), 2(e) show the receptance of beam when $n_2 = 1$. Figs. 2(b), 2(d), 2(f) show the receptance of beam when the varying ratios of material properties $n_2 = 3$. As can be seen from Figs. 2(a) and 2(b), when the forcing frequency is equal to the first natural frequency, the receptance matrices in both cases are maximum at the middle of the beam. When the forcing frequency is equal to the second natural frequency, the receptance matrices are maximum at the positions of $L/4$ and $3L/4$ from the left end of the beam as can be observed from Figs. 2(c) and 2(d). While, the receptance matrices are minimum at the middle of beam. However, the peaks in two cases $n_2 = 1$ and $n_2 = 3$ are different: the difference of two peaks in the case $n_2 = 1$ are larger than the case of $n_2 = 3$. This can be explained that the cross section at the two peaks in the case $n_2 = 1$ are far more different than the case $n_2 = 3$ resulting in the larger difference between the two peaks of the case $n_2 = 1$ in comparison with the case $n = 3$. Figs. 2(e) and 2(f) show the receptance matrices in two cases when the forcing frequency is equal to the third natural frequency. As presented, the receptances are maximum at the positions of about $L/6$, $3L/6$ and $5L/6$, while they are minimum at the positions of $2L/6$ and $4L/6$. Similar to the case when the forcing frequency is equal to the second natural frequency, the peaks of the receptance in the case of the linearly varying parameters is

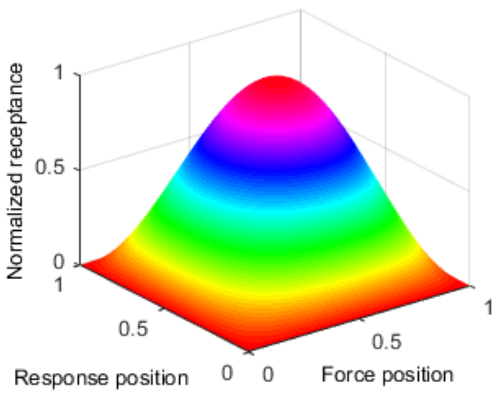

(a) $n_2 = 1, \omega = \omega_1$

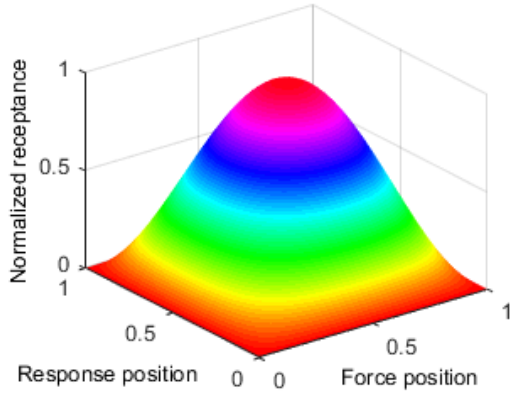

(b) $n_2 = 3, \omega = \omega_1$

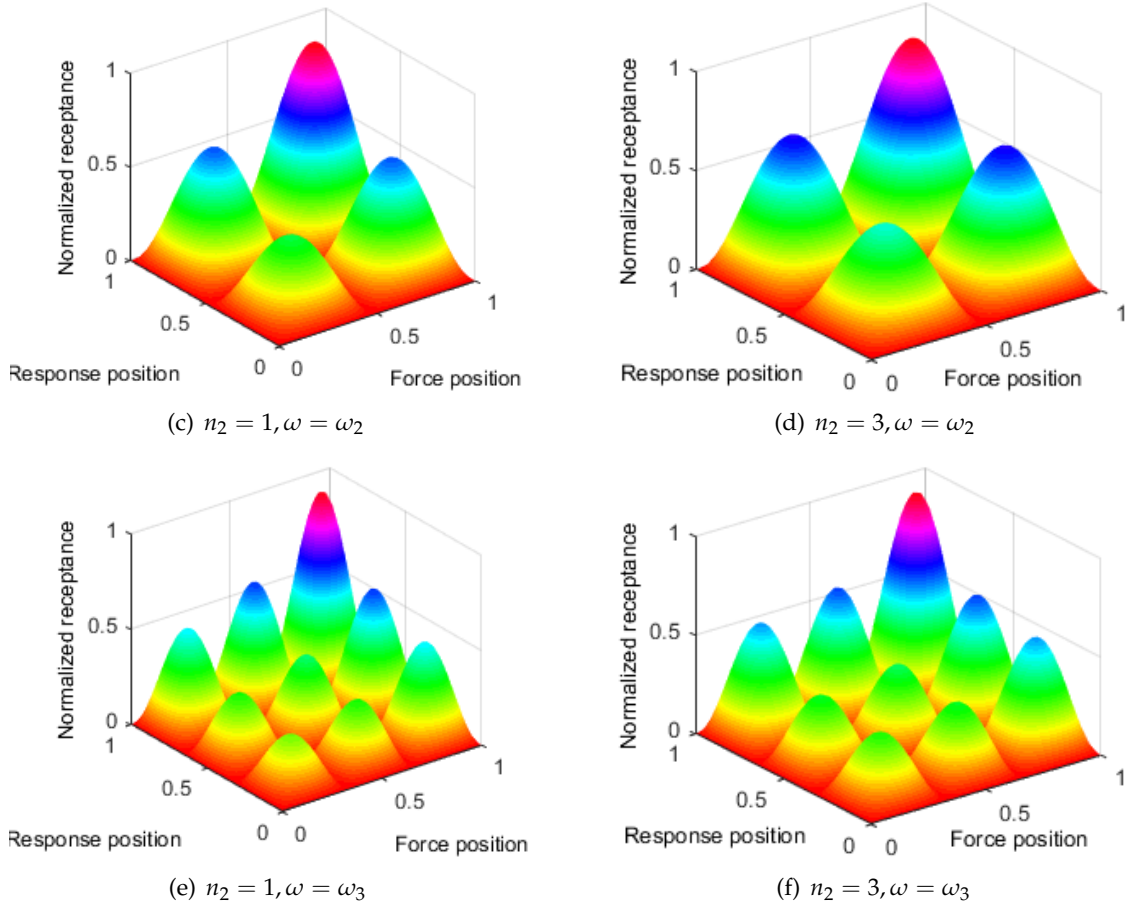

(c) $n_2 = 1, \omega = \omega_2$ (d) $n_2 = 3, \omega = \omega_2$

(e) $n_2 = 1, \omega = \omega_3$ (f) $n_2 = 3, \omega = \omega_3$

Fig. 2. Receptance matrices of AFG beam when the width varies

smaller than that of nonlinearly varying parameters. It is concluded that, the positions of maxima and minima of the receptances obtained at any natural frequency coincide with the positions of maxima and minima of the corresponding mode shape.

In order to give a clearer comparison of the differences between two peaks in the two cases $n_2 = 1$ and $n_2 = 3$, the receptance curves, when the force is fixed at the position of $L/3$, are extracted and presented in 2D graph as shown in Fig. 3. The force position of $L/3$ is chosen to ensure that the excitation is not applied at the nodes of receptance. Fig. 3(a) shows the receptance curve when the forcing frequency is equal to the first natural frequency. The peak of receptance in the case $n_2 = 3$ moves slightly to the left end of beam in comparison with the case $n_2 = 1$. As can be seen in Figs. 3(b) and 3(c), when the forcing frequency is equal to the second and third natural frequencies, the difference of two peaks in the case $n_2 = 1$ is higher than the case $n_2 = 3$ as mentioned.

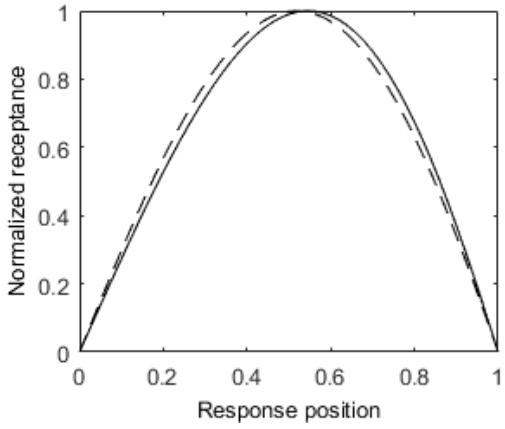

(a) $\omega = \omega_1$

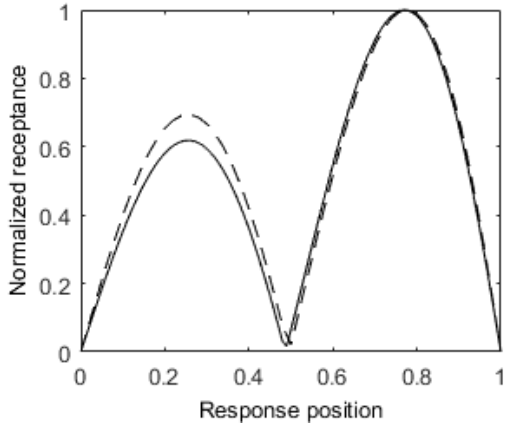

(b) $\omega = \omega_2$

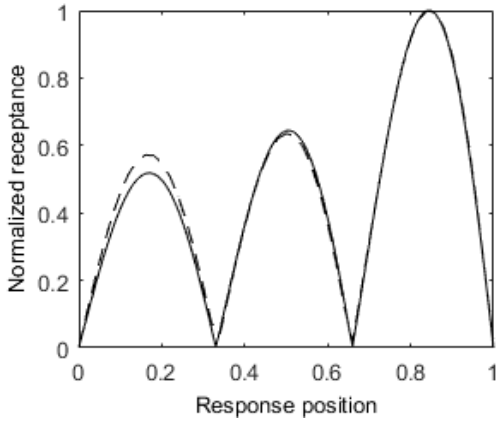

(c) $\omega = \omega_3$

Fig. 3. Receptance curves of beams without attached mass (Solid line: $n_2 = 1$; Dotted line: $n_2 = 3$)

3.3. Influence of the concentrated masses and the varying properties of material on the receptance

In this paper, two equal concentrated masses of 0.6 kg are attached on the simply supported AFG beam in the case $n_2 = 3$ in seven scenarios as listed in Table 2. The receptance matrices are calculated at 100 points spaced equally on the beam while the force moves along these points.

The receptance matrices of the AFG beams are changed when there are concentrated masses. Figs. 4(a) and 4(b) present the 3D and 2D graphs of the receptance of AFG beam carrying a mass at position $3L/4$ when the forcing frequency is equal to the first natural frequency of the beam-mass system. The influence of the mass on the receptance matrices

Table 2. Seven scenarios of attached masses

Scenario	ω	Position of m_1	Position of m_2
1	$\omega = \omega_1$	$3L/4$	-
2	$\omega = \omega_2$	$3L/4$	-
3	$\omega = \omega_3$	$L/6$	-
4	$\omega = \omega_3$	$3L/6$	-
5	$\omega = \omega_3$	$5L/6$	-
6	$\omega = \omega_3$	$L/6$	$3L/6$
7	$\omega = \omega_3$	$L/6$	$5L/6$

is small so that it is difficult to be observed from 3D graph in Fig. 4(a). However, the influence of the mass on the receptance can be inspected visually as presented in Fig. 4(b) when the receptance curves are extracted with the force applied at $0.5L$. When there is an attached mass at $3L/4$ the peak of receptance moves to the right side of the beam where the mass is attached.

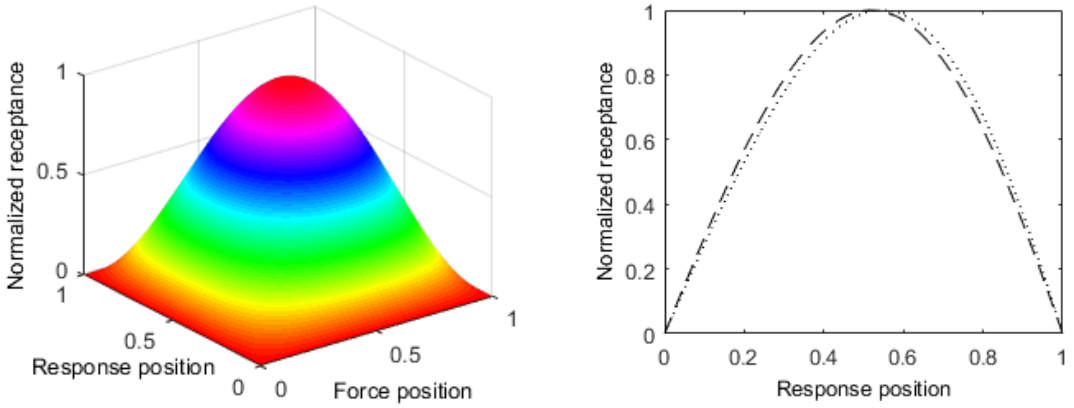

(a) Receptance matric (b) Receptance curve

Fig. 4. Receptance of AFG beam when $\omega = \omega_1$, mass position: $3L/4$
(Dotted line: without mass; Dashed line: attached mass)

When the mass is attached at the position of $3L/4$ and the forcing frequency is equal to the second natural frequency, the peak at the mass position is pressed down significantly. The node of the receptance curve moves toward the right of beam where the mass is attached as can be observed from Figs. 5(a) and 5(b). Figs. 6 illustrate the 2D and 3D graphs of the receptance of AFG beam when the mass is attached at $L/6$, $L/2$ and $5L/6$ and the forcing frequency is equal to the third natural frequency of the beam-mass system. As can be seen from these graphs, the peaks at the mass position are dropped remarkably and peaks of the receptance move to the side where the mass is attached.

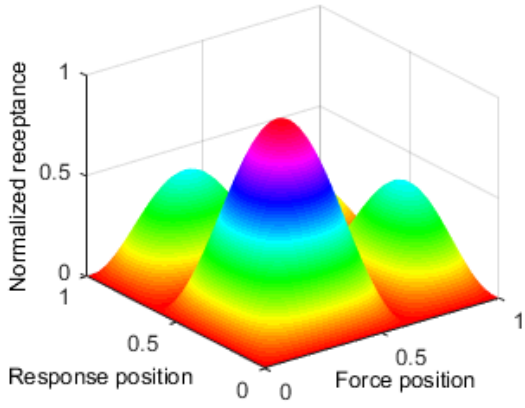

(a) Receptance matric

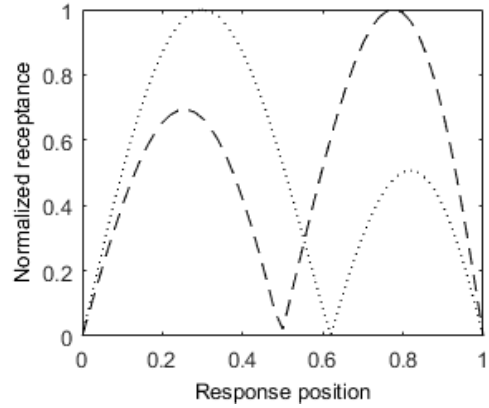

(b) Receptance curve

Fig. 5. Receptance of AFG beam when $\omega = \omega_2$, mass position: $3L/4$
(Dotted line: without mass; Dashed line: attached mass)

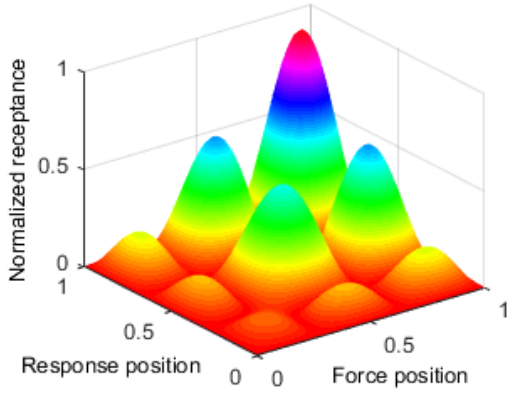

(a) Receptance matric, mass position $L/6$

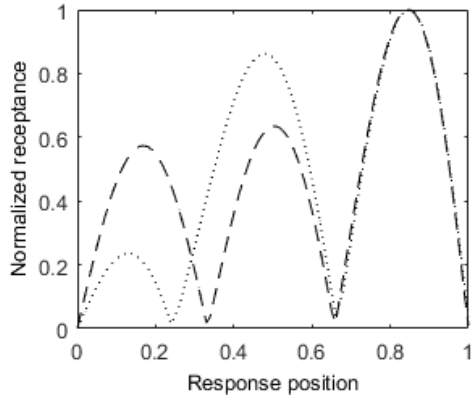

(b) Receptance curve, mass position $L/6$

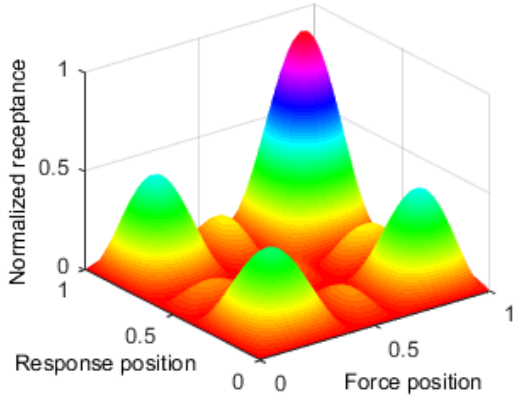

(c) Receptance matric, mass position $L/2$

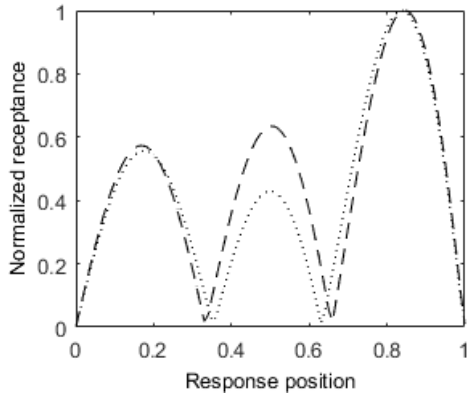

(d) Receptance curve, mass position $L/2$

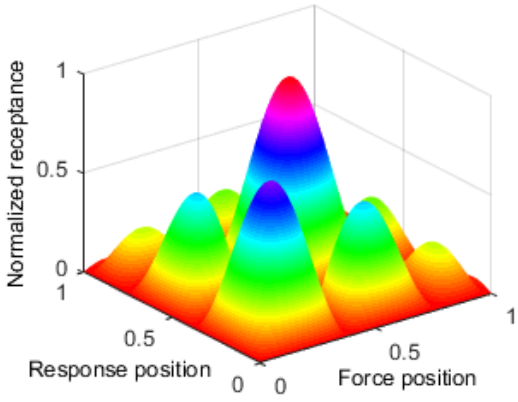

(e) Receptance matric, mass position $5L/6$

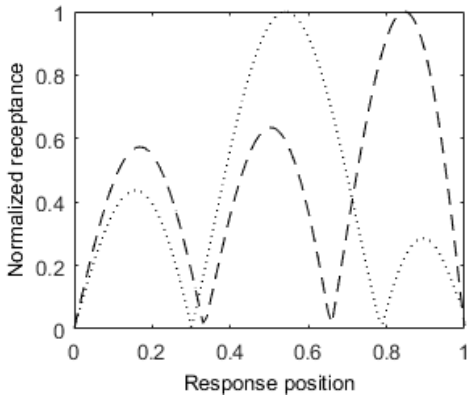

(f) Receptance curve, mass position $5L/6$

Fig. 6. Receptance of AFG beam when $\omega = \omega_3$
(Dotted line: without mass; Dashed line: attached mass)

When two masses are located at the two peaks of receptance and the forcing frequency is equal to the third natural frequency of the beam-mass system, the peaks corresponding to these positions decrease as demonstrated in Fig. 7. Figs. 7(a) and 7(b) present the receptance of beam when two masses are located at the positions of $L/6$ and $3L/6$. As can be observed from these graphs, the peaks corresponding to these positions decrease significantly and peaks and nodes of the receptance curve moves to the left side where the two masses are attached. When two masses are located at the positions of $L/6$ and $5L/6$, four peaks corresponding to these positions decrease significantly as shown in the Figs. 7(c) and 7(d). It is noted that the first node of receptance moves clearly to the first mass position which is close to that node and the second node moves to the second mass position.

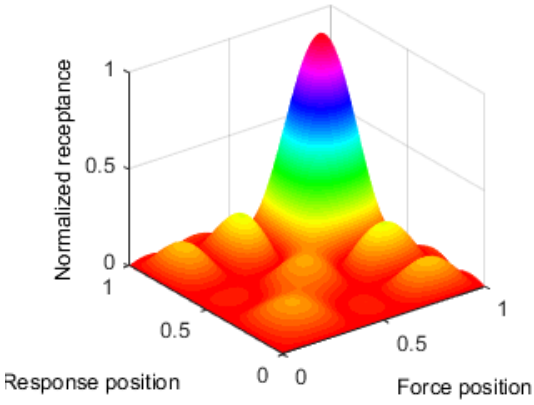

(a) Receptance matric, masses at $L/6$ and $L/2$

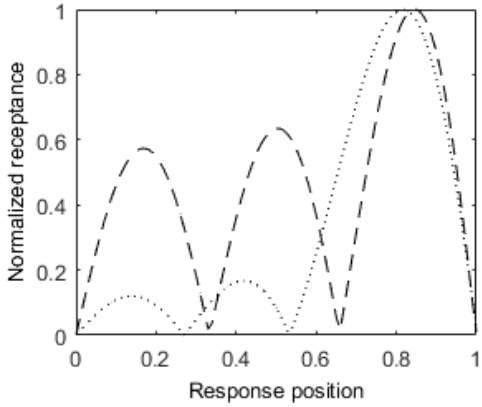

(b) Receptance, masses at $L/6$ and $L/2$

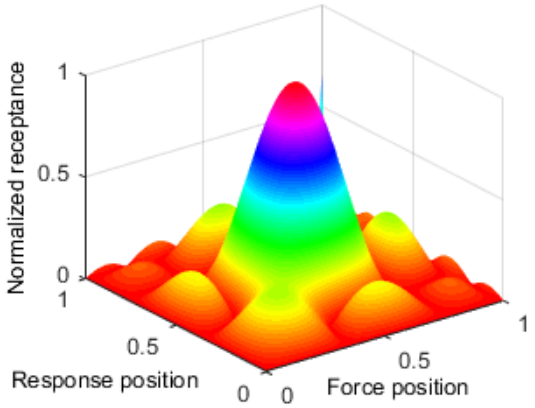

(c) Receptance matric, masses at $L/6$ and $5L/6$

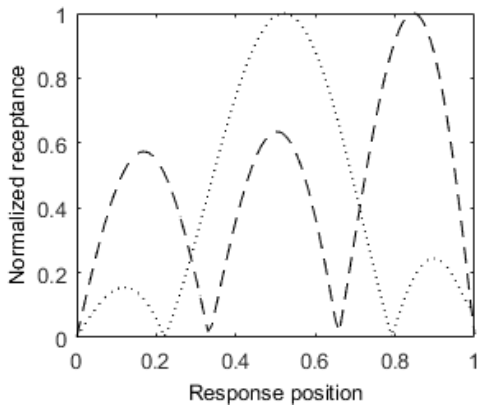

(d) Receptance, masses at $L/6$ and $5L/6$

Fig. 7. Receptance of AFG beam when $\omega = \omega_3$, two masses are attached (Dotted line: without mass; Dashed line: attached masses)

4. CONCLUSION

In this paper, the exact formula of receptance function of a tapered AFG beam with varying parameters given in the form of an arbitrary order polynomial is presented. When the term $(EI)'/EI$ and $(EI)''/EI$ cannot be expressed as a geometric series as presented in published works, they will be expressed as a converged alternative power series. The numerical simulations of receptance of the simply supported nonlinear AFG beam as an example are provided.

Numerical results show that when the exciting frequency is equal to the natural frequencies, the maximum and minimum positions of the receptances are the same with the maxima and minima positions of the corresponding mode shapes. The influence of the concentrated masses on the receptance of the AFG beam is also investigated. When there are concentrated massese, the shape of receptance of the tapered AFG beam is changed. The peaks of receptance at the positions of attached masses decrease. The peaks and nodes of the receptance of the AFG beam tend to move toward the mass positions. The simulation results in this work can be used to validate future work using other methods and they can be useful for controlling the vibration amplitude at some specific points along the beam by applying concentrated masses.

DECLARATION OF COMPETING INTEREST

The authors declare that they have no known competing financial interests or personal relationships that could have appeared to influence the work reported in this paper.

ACKNOWLEDGEMENT

This research is funded by Vietnam Academy of Science and Technology under grant number ĐLTE00.03/23-24.

REFERENCES

[1] M. Ghandchi Tehrani, R. N. R. Elliott, and J. E. Mottershead. Partial pole placement in structures by the method of receptances: Theory and experiments. *Journal of Sound and Vibration*, **329**, (2010), pp. 5017–5035. https://doi.org/10.1016/j.jsv.2010.06.018.

[2] J. E. Mottershead. On the zeros of structural frequency response functions and their sensitivities. *Mechanical Systems and Signal Processing*, **12**, (1998), pp. 591–597. https://doi.org/10.1006/mssp.1998.0167.

[3] Z. Wang, R. M. Lin, and M. K. Lim. Structural damage detection using measured FRF data. *Computer Methods in Applied Mechanics and Engineering*, **147**, (1997), pp. 187–197. https://doi.org/10.1016/s0045-7825(97)00013-3.

[4] M. Gürgöze and H. Erol. Determination of the frequency response function of a cantilevered beam simply supported in-span. *Journal of Sound and Vibration*, **247**, (2001), pp. 372–378. https://doi.org/10.1006/jsvi.2000.3618.

[5] Q. Huang, Y. L. Xu, J. C. Li, Z. Q. Su, and H. J. Liu. Structural damage detection of controlled building structures using frequency response functions. *Journal of Sound and Vibration*, **331**, (2012), pp. 3476–3492. https://doi.org/10.1016/j.jsv.2012.03.001.

[6] L. Li, Y. Hu, X. Wang, and L. Lü. A hybrid expansion method for frequency response functions of non-proportionally damped systems. *Mechanical Systems and Signal Processing*, **42**, (2014), pp. 31–41. https://doi.org/10.1016/j.ymssp.2013.07.020.

[7] G. Failla. An exact generalised function approach to frequency response analysis of beams and plane frames with the inclusion of viscoelastic damping. *Journal of Sound and Vibration*, **360**, (2016), pp. 171–202. https://doi.org/10.1016/j.jsv.2015.09.006.

[8] K. V. Nguyen, T. T. B. Dao, and M. Van Cao. Comparison studies of the receptance matrices of the isotropic homogeneous beam and the axially functionally graded beam carrying concentrated masses. *Applied Acoustics*, **160**, (2020). https://doi.org/10.1016/j.apacoust.2019.107160.

[9] K. V. Singh, C. Black, and R. Kolonay. Active aeroelastic output feedback control with partial measurements by the method of receptances. *Aerospace Science and Technology*, **86**, (2019), pp. 47–63. https://doi.org/10.1016/j.ast.2018.12.037.

[10] S. Lenci, F. Clementi, and C. E. N. Mazzilli. Simple formulas for the natural frequencies of non-uniform cables and beams. *International Journal of Mechanical Sciences*, **77**, (2013), pp. 155–163. https://doi.org/10.1016/j.ijmecsci.2013.09.028.

[11] R. Eberle and M. Oberguggenberger. A new method for estimating the bending stiffness curve of non-uniform Euler-Bernoulli beams using static deflection data. *Applied Mathematical Modelling*, **105**, (2022), pp. 514–533. https://doi.org/10.1016/j.apm.2021.12.042.

[12] S. Hadian Jazi, M. Hadian, and K. Torabi. An exact closed-form explicit solution of free transverse vibration for non-uniform multi-cracked beam. *Journal of Sound and Vibration*, **570**, (2024). https://doi.org/10.1016/j.jsv.2023.117986.

[13] Q. S. Li. Free vibration analysis of non-uniform beams with an arbitrary number of cracks and concentrated masses. *Journal of Sound and Vibration*, **252**, (2002), pp. 509–525. https://doi.org/10.1006/jsvi.2001.4034.

[14] M. A. Mahmoud. Natural frequency of axially functionally graded, tapered cantilever beams with tip masses. *Engineering Structures*, **187**, (2019), pp. 34–42. https://doi.org/10.1016/j.engstruct.2019.02.043.

[15] M. A. Mahmoud. Free vibrations of tapered and stepped, axially functionally graded beams with any number of attached masses. *Engineering Structures*, **267**, (2022). https://doi.org/10.1016/j.engstruct.2022.114696.

[16] G. Tan, Y. Liu, Y. Gong, Y. Shen, and Z. Liu. Free vibration of the cracked non-uniform beam with cross section varying as polynomial functions. *KSCE Journal of Civil Engineering*, **22**, (2018), pp. 4530–4546. https://doi.org/10.1007/s12205-018-1833-5.